INDERSCIENCE PUBLISHERS
Linking academia, business and industry through research

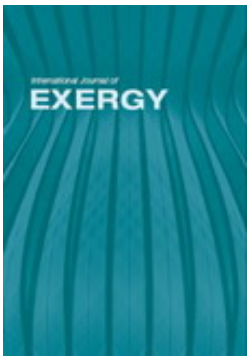

International Journal of Exergy

ISSN online: 1742-8300 - ISSN print: 1742-8297
https://www.inderscience.com/ijex

Exergetic comparison of a novel to a conventional small-scale power-to-ammonia cycle

Pascal Koschwitz, Daria Bellotti, Cheng Liang, Bernd Epple

DOI: 10.1504/IJEX.2023.10058600

Article History:

Received:	24 March 2023
Last revised:	25 March 2023
Accepted:	27 April 2023
Published online:	30 October 2023

Exergetic comparison of a novel to a conventional small-scale power-to-ammonia cycle

Pascal Koschwitz*

Institute for Energy Systems and Technology,
Technical University of Darmstadt,
Otto-Berndt-Str. 2, 64287 Darmstadt, Germany
Email: pascal.koschwitz@est.tu-darmstadt.de
*Corresponding author

Daria Bellotti

Thermochemical Power Group,
Dipartimento di Macchine Sistemi Energetici e Trasporti,
University of Genova,
Via Montallegro 1, 16145 Genova, Italy
Email: daria.bellotti@unige.it

Cheng Liang

Proton Ventures B.V.,
Karel Doormanweg 5, NL-3115, JD,
Schiedam, The Netherlands
Email: cheng.liang@protonventures.com

Bernd Epple

Institute for Energy Systems and Technology,
Technical University of Darmstadt,
Otto-Berndt-Str. 2, 64287 Darmstadt, Germany
Email: bernd.epple@est.tu-darmstadt.de

Abstract: Green ammonia is a promising carbon-free energy vector and means to store hydrogen efficiently. Employing the software Aspen Plus®, this work presents an exergetic comparison of a novel small-scale power-to-ammonia system, to be tested in 2023 and designed for low investment cost and dynamic flexibility, to a conventional system. For a thorough evaluation six equations of state, one provided by an industry partner, as well as chemical exergies with and without excess values are compared. With 64.59%, the novel design has a 4.87% lower exergetic degree of efficiency. The difference can be attributed to the simplified design of the novel cycle, mainly to the use of an electrical preheater instead of an internal gas-gas heat exchanger and a recycle valve instead of a recycle compressor. However, an upcoming exergy economic analysis will show that the novel cycle is more economical overall, as its investment costs are lower.

Keywords: exergy analysis; power-to-ammonia; P2A; process design comparison; Aspen Plus® process simulation.

Reference to this paper should be made as follows: Koschwitz, P., Bellotti, D., Liang, C. and Epple, B. (2023) 'Exergetic comparison of a novel to a conventional small-scale power-to-ammonia cycle', *Int. J. Exergy*, Vol. 42, No. 2, pp.127–158.

Biographical notes: Pascal Koschwitz holds an MSc in Process Engineering from the Technical University of Berlin, Germany. He is currently a PhD candidate at the Institute for Energy Systems and Technology, Technical University of Darmstadt, Germany.

Daria Bellotti holds an MSc and PhD in Mechanical Engineering at the University of Genova, Italy. She is currently an Assistant Professor at the Thermochemical Power Group, University of Genova, Italy.

Cheng Liang holds an MSc in Mechanical Engineering from the Technical University of Delft, The Netherlands. She is currently working as a Process and Innovation Engineer at Proton Ventures B.V., The Netherlands.

Bernd Epple holds a Dipl-Ing degree and PhD in Mechanical Engineering from Stuttgart University, Germany. Since 2004, he is the Head of the Institute for Energy Systems and Technology at the Technical University of Darmstadt, Germany.

1 Introduction

After sulphuric acid ammonia is the world's most produced chemical in terms of tons per year, of which 80% are used for fertilisers (Bazzanella et al., 2017). The growth of the world's population and ammonia production correlate (Appl, 2000a). But a growing world population only exacerbates the problem of manmade climate change. Therefore, it is not without irony that ammonia is being suggested as a green energy vector to replace fossil fuels.

The Haber-Bosch reaction is the most common way to produce ammonia. It is a gaseous equilibrium reaction of hydrogen (H_2) and nitrogen (N_2) in a ratio of three to one to form two ammonia (NH_3) molecules in the presence of a solid catalyst. The equilibrium equation which has a negative reaction enthalpy is shown in equation (1) at standard conditions (25°C and 1.01325 bar) (Bazzanella et al., 2017).

$$1.5H_{2(g)} + 0.5N_{2(g)} \rightleftharpoons NH_{3(g)} \quad \Delta\bar{h}^{\circ} = -46.22 \text{ kJ} / \text{mol}_{NH_3} \tag{1}$$

Older and newer ways than Haber-Bosch for nitrogen fixation in ammonia exist (Patil et al., 2000; Wang et al., 2018; Renner et al., 2015; Travis, 2018), but are not industrially relevant.

The most common feedstock in the Haber-Bosch process are natural gas and air with the undesired by product carbon-dioxide (Appl, 2000b). Thus, efforts are being undertaken to turn the Haber-Bosch process green. Such green power-to-ammonia (P2A) processes use green electricity to power water electrolysis units to yield H_2 and air separation units to yield N_2. In academia, green ammonia production (Bañares-Alcántara

et al., 2015; Inamuddin et al., 2020; Valera-Medina and Banares-Alcantara, 2021) and the use of ammonia as a carbon-free energy vector (Valera-Medina et al., 2018; Elishav et al., 2020; Morlanés et al., 2021) is being discussed increasingly. Furthermore, there exist several recent, current and planned research projects, e.g., in the UK where Siemens has built a small-scale P2A reactor with a conventional catalyst (Siemens Energy, 2020) or in Japan at the Fukushima Renewable Energy Institute where a 100% ammonia fuelled gas turbine with an electrical output of 41.8 kW has been successfully run for the first time worldwide (Kobayashi, 2014). In addition to academia and research, there are numerous ongoing renewable ammonia industry projects. In Australia, the 15 GW Asian Renewable Energy Hub, a 6,500 square kilometre wind and solar farm, is planned to produce and export green ammonia starting in 2028 (Brown, 2020; Tancock, 2020). And only very recently EverWind from Canada and Uniper from Germany have reached a deal to produce half a million tonnes of green ammonia annually in Nova Scotia to be shipped to Germany starting in 2025 (Uniper SE, 2022).

A first adopter of ammonia as a fuel is likely the maritime industry as ammonia is shipped worldwide already and using it as both cargo and fuel seems logical (Teo, 2020). MAN is developing ammonia retrofits for their two-stroke diesel engines (Jacobsen, 2020) and the shipping company NYK LINE is developing ammonia fuelled tug boats and ammonia carriers (Taruishi, 2020).

This work compares a novel to a conventional small-scale 15 kW P2A cycle. The novel cycle, developed in the EU FLEXnCONFU project, was introduced in Koschwitz et al. (2022b) with a thermodynamic steady state energetic analysis and optimisation. The new cycle's predicted dynamic behaviour was analysed in Koschwitz et al. (2022a, 2023). The containerised solution of the novel cycle is under construction and will be tested at the University of Genova in 2023.

Small-scale P2A can be a valuable means in remote or islanded areas to store energy (Rouwenhorst et al., 2019; Bañares-Alcántara et al., 2015) and to use the ammonia as a fertiliser (Reese et al., 2016; Lin et al., 2020). Another advantage of small-scale compared to big scale is its relatively fast start-up time to match the fluctuations in the renewables (Verleysen et al., 2021).

The motivation for an exergetic comparison in this work is threefold. First, only exergy can compare the efficiency of energy storage systems fairly, as not only the first but also the second law of thermodynamics is taken into consideration. It is the aim to show that the novel cycle exergetically compares to a conventional small-scale Haber-Bosch design. Second and third, an exergy analysis lays the foundation for both an exergetic costing (Tsatsaronis and Winhold, 1985; Bejan et al., 1996; Lazzaretto and Tsatsaronis, 2006) and exergetic environmental analysis (Meyer, 2006; Meyer et al., 2009; Tsatsaronis and Morosuk, 2008a, 2008b), the former showing whether a process is economical, the latter whether it is ecological. Both an exergetic costing and environmental comparison analysis of the two designs are planned as future works, for which this work lays the foundation.

2 System description

The novel and conventional P2A process diagrams are displayed in Figure 1 and Figure 2. The streams are numbered H_2, N_2 and in roman letters I to XII. The 15 kW electrolyser splits water to provide H_2. The N_2 from the air is provided by e.g., membrane

separation. In the novel layout, the inlets H_2 and N_2 enter the system (dotted system boundary) and are mixed with the recycle XII in the mixer (M-1) at 8 barg. The outlet I of M-1 enters the compressor (C-1), which is driven by electric power $P_{el,C-1}$ to increase the pressure to 80 barg (s. Figure 1). In contrast, in the conventional layout the mixing of the inlets and recycle takes place at 80 barg after the first compressor C-1 (s. Figure 2). Thus, in the conventional layout C-1 only compresses the inlets to 80 barg, which are then mixed with the recycle XII in M-1 at 80 barg (s. Figure 2). For a better overview, all the differences of the two layouts mentioned in this section are listed in Table 1.

In the novel layout, the compressor outlet II enters the electric heat exchanger (E-1), which takes up the electric power $P_{el,E-1}$ and increases the temperature to the optimal reactor inlet temperature of 380°C (s. Figure 1). In contrast, in the conventional design the compressor outlet enters the internal gas-gas heat exchanger E-1 to leave with a temperature of 213°C (s. Figure 2 and Table 1). The heat provided in E-1 is provided by the reactor outlet stream VI.

In the novel layout, the preheated outlet III enters R-1, the first of three identical fixed-bed reactor sections (R-1, R-2 and R-3). Each section is temperature controlled by a combination of air cooling and electric heating to ensure the optimal temperature profile for NH_3 conversion of 380°C, 350°C and 340°C (s. Figure 1), as discussed by Koschwitz et al. (2022b). The electric power uptake and given-off heat stream of each section is $P_{el,R-1}$, $P_{el,R-2}$ and $P_{el,R-3}$ and $\dot{Q}_{R-1}$, $\dot{Q}_{R-2}$ and $\dot{Q}_{R-3}$. In contrast, as will be discussed in Section 4.3, in the conventional layout the optimal temperature profile is slightly different with 380°C, 360°C and 340°C. In other words, only the temperature in R-2 is higher by 10°C (s. Figure 2 and Table 1).

In the novel layout, the outlet VI of R-3 enters the condenser (V-1), which takes up the electric power $P_{el,V-1}$ to cool VI to 15°C. Here, for simplicity, a worst-case vapour compression refrigeration (VCR) with a coefficient of performance (COP) of 1 is assumed. In contrast, in the conventional layout the reactor outlet VI is used in the internal gas-gas heat exchanger E-1 to heat up the reactor inlet III (s. Figure 2). The cooled down reactor outlet VI-2 then enters V-1.

In both layouts, the outlets of V-1 are the liquid stream VII and the gaseous stream VIII. VII mainly consists of NH_3 and exits the system to the ammonia storage tank. VIII, which mainly consists of unconverted H_2 and N_2, enters the splitter (S-1). In the real test plant, the purging of the system via the purge valve (I-1) will take place intermittently and depends on the measured concentration of unwanted inerts that enter the cycle such as Argon. For simplicity, S-1 is assumed to have a split ratio for VIII of 0.05 and 99.95 mol% for IX and XI. IX enters I-1. The purge X exits both I-1 and the system.

In the novel layout XI enters the recycle valve (I-2). The outlet XII of I-2 is the recycle stream, which has a reduced pressure of 8 barg to match the low pressure of the inlets H_2 and N_2 to close the cycle in M-1. In contrast, in the conventional layout the pressure is not reduced. Instead, a second recycle compressor (C-2) compensates for the pressure losses in the previous components (s. Figure 2). The outlet XII of C-2 has a pressure of 80 barg to match the outlet pressure of the inlet compressor C-1.

Figure 1 Flowsheet of the novel P2A cycle

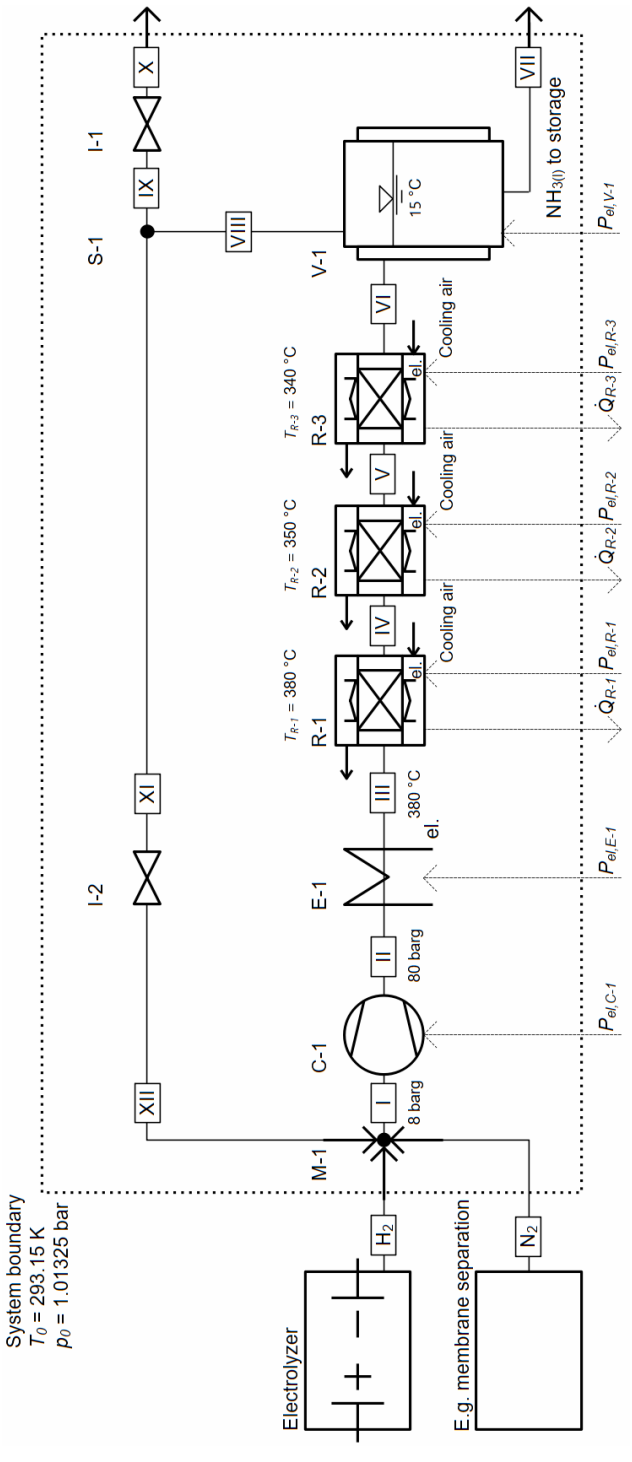

Figure 2 Flowsheet of a conventional P2A cycle

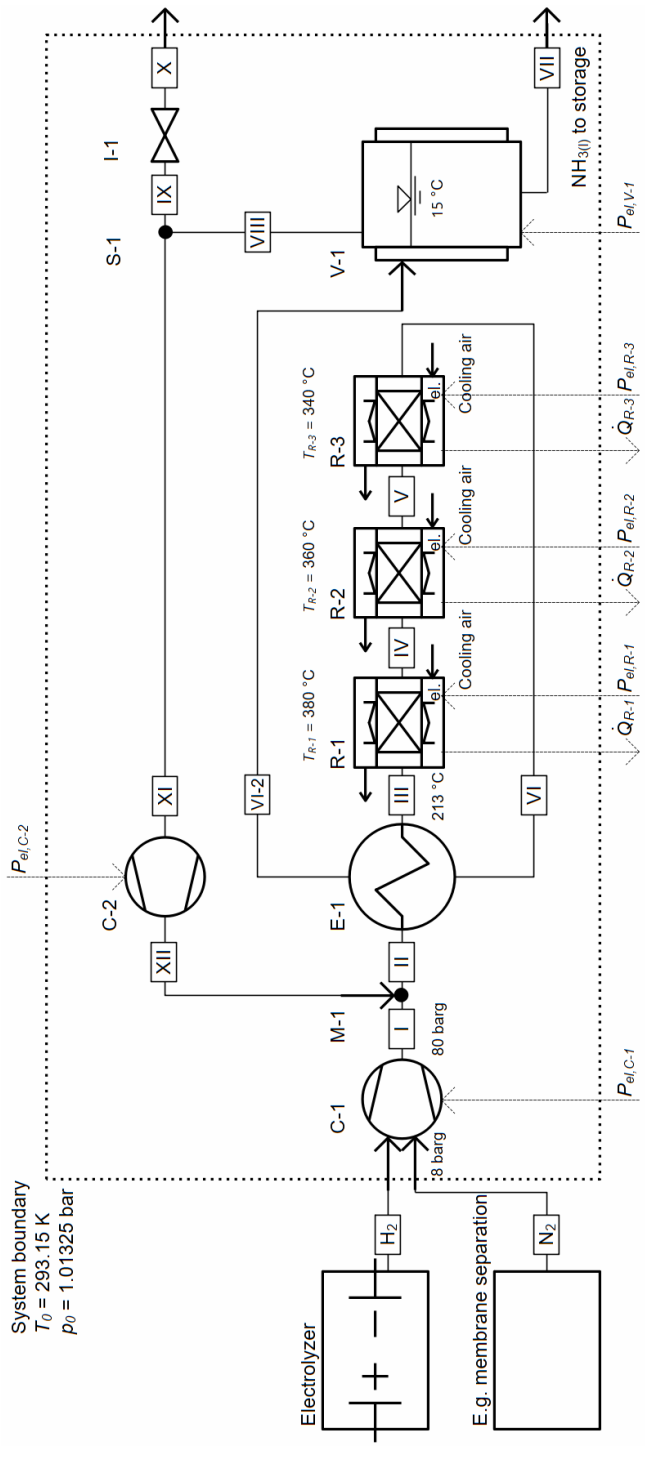

Table 1 Main differences of the novel and conventional P2A cycle

Difference	*Novel P2A cycle*	*Conventional P2A cycle*
M-1 mixer	The mixing of the educts H_2 and N_2 as well as the recycle XII takes place before the compressor C-1 at 8 barg.	The mixing of the recycle and educts takes place after the compressor C-1 at 80 barg.
C-1 compressor	The compressor inlets are the educts H_2 and N_2 as well as the recycle XII. The novel cycle only has one compressor, C-1.	The compressor inlets are only the educts H_2 and N_2. The conventional cycle has the inlet compressor C-1 as well as a recycle compressor C-2.
E-1 heater	The heater E-1 is an electrical heater that heats up the reactor inlet III to 380°C.	The heater E-1 is an internal gas-gas heat exchanger that heats up the reactor inlet III to 213°C.
Reactor temperature profile	The reactor compartments R-1, R-2 and R-3 are isothermal temperature controlled at 380°C, 350°C and 340°C.	The reactor compartments R-1, R-2 and R-3 are isothermal temperature controlled at 380°C, 360°C and 340°C.
Recycle	The pressure in the recycle is reduced via the recycle valve I-2 to match the low pressure of 8 barg of the inlets.	The pressure in the recycle is maintained at 80 barg by the recycle compressor C-2, which compensates for the pressure losses in the upstream cycle components.

For conventional ammonia cycles both the use of a recycle compressor (see for example, (Appl, 2000b, 2000c; Verleysen et al., 2020, 2021; Bland, 2015; Aspen Tech, 2015; Tripodi et al., 2018; Stephens and Richards, 1973; Araújo and Skogestad, 2008; Zhang et al., 2010; Tian et al., 2011; Palys et al., 2018; Kirova-Yordanova, 2004; Penkuhn and Tsatsaronis, 2017) and the use of an internal gas-gas heat exchanger (see for example, Appl, 2000b, 2000c; Reese et al., 2016; Verleysen et al., 2021; Bland, 2015; Aspen Tech, 2015; Stephens and Richards, 1973; Araújo and Skogestad, 2008; Zhang et al., 2010; Tian et al., 2011; Palys et al., 2018; Verleysen et al., 2020; Kirova-Yordanova, 2004; Morud and Skogestad, 1998; Kasiri et al., 2003; Bothinah et al., 2016; Allman and Daoutidis, 2018; Jinasena et al., 2018; Adhi and Prasetyo 2018) are widespread. From an exergetic point of view, the use of both components is likely to be superior to the proposed recycle valve and the electrical heater in the novel layout. However, from an investment cost point of view the opposite can be assumed. As necessary preliminary work for an exergy costing comparison, this work shall determine the extend to which the two layout differences affect the exergetic parameters of the cycles, cycle components and cycle streams. For this, since only the differences matter, the system boundary excludes the input sources, i.e., electrolyser and N_2-source, which are the same in both layouts. The unit operations R-1, R-2, R-3, V-1, S-1 and I-1 are also the same in both layouts. However, because they are downstream and affected by the upstream layout differences, they are included in the system boundary.

3 Methods

To derive the thermodynamic data for the exergy analyses the simulation environment Aspen Plus® (Aspen Tech, 2023) is employed. In Section 3.1 the key aspects of the exergetic approach are explained. In Section 3.2 the simulation setup is reported. The three goals of the simulation setup are described in Subsections 3.2.1, 3.2.2 and 3.2.3.

3.1 Exergy analysis

The exergy concept (Bejan et al., 1996; Szargut et al., 1988; Moran et al., 2014; Tsatsaronis, 2007) is a strong and long-established tool for the evaluation of power and chemical systems to determine inefficiencies and ways to reduce them. As opposed to a pure energetic analysis, exergy is that theoretical maximum part of energy that can be converted to power. Since P2A processes, like all other power-to-X-to-power processes, use power and generate it again, it is more sensible to look at exergy and not only energy. Perhaps even more or equally important, an exergy analysis includes an entropy analysis. Exergy destruction, i.e., potential power lost through inefficiencies in cycle components, is proportional to entropy production. Therefore, an exergetic analysis determines the exergy destruction in a process and thus reveals the inefficiencies of that process in a way that a pure energetic analysis cannot.

The exergy concept has been applied to ammonia production processes already (Kirova-Yordanova, 2004; Penkuhn and Tsatsaronis, 2017; Radgen and Lucas, 1996). Neglecting kinetic and potential energy, the exergy stream $\dot{E}_i$ of a stream *i* is the sum of its physical $\dot{E}_i^{PH}$ and chemical exergy $\dot{E}_i^{CH}$ stream, shown in equation (2).

$$\dot{E}_i = \dot{E}_i^{PH} + \dot{E}_i^{CH} \tag{2}$$

The chemical exergy concept is explained, e.g., in Bejan et al. (1996) and Sato (2004). The molar chemical exergy of a mixture $\overline{e}_{Mix}^{CH}$ is the sum of the ideal molar chemical exergy $\overline{e}_{Mix,id}^{CH}$ and the molar excess Gibbs energy $\overline{g}_{Mix}^{e}$, shown in equation (3) (Sato, 2004).

$$\overline{e}_{Mix}^{CH} = \underbrace{\sum_{j=1}^{n} y_j \overline{e}_j^{CH} + T_0 \overline{R} \sum_{j=1}^{n} y_j \ln\left(y_j\right)}_{=\overline{e}_{Mix,id}^{CH}} + \overline{g}_{Mix}^{e} \tag{3}$$

In equation (3), y_j is the molar fraction and $\overline{e}_j^{CH}$ the chemical exergy of the j^{th} component H_2, N_2 or NH_3. In this work the values for $\overline{e}_j^{CH}$ are taken from Szargut et al. (1988). $\overline{g}_{Mix}^{e}$ from equation (3) can be calculated by subtracting the ideal $\overline{g}_{Mix,id}$ from the real Gibbs energy of the mixture $\overline{g}_{Mix}$, given in equation (4).

$$\overline{g}_{Mix}^{e} = \overline{g}_{Mix} - \overline{g}_{Mix,id} \tag{4}$$

$\overline{g}_{Mix}^{e}$ from equation (4) is calculated by determining $\overline{g}_{Mix}$ and $\overline{g}_{Mix,id}$ in Aspen Plus® via the use of a non-ideal equation of state (EoS) and the ideal EoS respectively. In literature, (chemical) exergies for ammonia processes are calculated in different ways. Bram and Ruyck (1997) employ Aspen Plus® with an external Fortran subroutine. An ideal mixture is assumed and only the chemical exergies of hydrocarbons are considered. Kirova-Yordanova (2004) conducts an exergetic analysis of ten designs of ammonia synthesis loops at 300 bar. The mixtures are treated as real mixtures. Penkuhn and Tsatsaronis (2017) evaluate two designs of ammonia synthesis loops with an advanced exergy analysis. Radgen and Lucas (1996) evaluate an ammonia and urea plant through an exergy analysis. Osuolale and Zhang (2018) use the excess approach from equation (3)

for the evaluation of a distillation system. For the evaluation of a water-ammonia absorption refrigeration system Gupta et al. (2015) employ the approach from equation (4).

The most important exergetic indicators in this work are $\dot{E}_{D,k}$, $\dot{E}_{D,tot}$, ϵ_k, ϵ_{tot}, ξ_k, ξ_{tot} and ϕ_k. The exergetic destruction $\dot{E}_{D,k}$ that takes place in each unit operation k is being calculated by subtracting the exergetic product $\dot{E}_{P,k}$ leaving from the exergetic fuel $\dot{E}_{F,k}$ entering that unit operation, given in equation (5).

$$\dot{E}_{D,k} = \dot{E}_{F,k} - \dot{E}_{P,k} \tag{5}$$

The total exergetic destruction $\dot{E}_{D,tot}$ for the whole system is the sum of all $\dot{E}_{D,k}$, given in equation (6).

$$\dot{E}_{D,tot} = \sum_{k=1}^{m} \dot{E}_{D,k} \tag{6}$$

The exergetic degree of efficiency of each unit operation ϵ_k is calculated by the ratio $\dot{E}_{P,k}$ to $\dot{E}_{F,k}$, given in equation (7).

$$\epsilon_k = \frac{\dot{E}_{P,k}}{\dot{E}_{F,k}} \tag{7}$$

The total exergetic degree of efficiency ϵ_{tot} is calculated by the ratio of the total exergetic product $\dot{E}_{P,tot}$ to fuel $\dot{E}_{F,tot}$, i.e., the sum of all $\dot{E}_{P,k}$ leaving to the sum of all $\dot{E}_{F,k}$ entering the system across the system boundary (*sb*), given in equation (8).

$$\epsilon_{tot} = \frac{\dot{E}_{P,tot}}{\dot{E}_{F,tot}} = \frac{\sum_{k=1}^{m} \dot{E}_{P,k}\big|_{sb}}{\sum_{k=1}^{m} \dot{E}_{F,k}\big|_{sb}} \tag{8}$$

The ratio of exergy destruction in a component to total exergetic fuel ξ_k is calculated by the ratio of $\dot{E}_{D,k}$ to $\dot{E}_{F,tot}$, given in equation (9).

$$\xi_k = \frac{\dot{E}_{D,k}}{\dot{E}_{F,tot}} = \frac{\dot{E}_{D,k}}{\sum_{k=1}^{m} \dot{E}_{F,k}\big|_{sb}} \tag{9}$$

Analogously, ξ_{tot} is calculated by the ratio of $\dot{E}_{D,tot}$ to $\dot{E}_{F,tot}$, given in equation (10).

$$\xi_{tot} = \frac{\dot{E}_{D,tot}}{\dot{E}_{F,tot}} = \frac{\sum_{k=1}^{m} \dot{E}_{D,k}}{\sum_{k=1}^{m} \dot{E}_{F,k}\big|_{sb}} \tag{10}$$

Lastly, the ratio of exergy destruction in a component to total exergy destruction ϕ_k is calculated by the ratio of $\dot{E}_{D,k}$ to $\dot{E}_{D,tot}$, given in equation (11).

$$\phi_k = \frac{\dot{E}_{D,k}}{\dot{E}_{D,tot}} = \frac{\dot{E}_{D,k}}{\sum_{k=1}^{m} \dot{E}_{D,k}} \tag{11}$$

Table 2 Novel and conventional layout main exergy and Aspen Plus® parameters

Exergy					
Chemical exergy model			Szargut et al. (1988)		
Reference temperature			25		°C
Reference pressure			1.01325		bar
Aspen Plus®					
Pressure drop per unit operation			1		mbar
Components			H_2, N_2 and NH_3		
EoS			HYSPR-mp used by industry partner (Koschwitz et al., 2022b)		
Modified binary interaction parameters of HYSPR-mp (Koschwitz et al., 2022b)		H_2	N_2	NH_3	
	H_2	/	–0.036	0	
	N_2	–0.036	/	0.222	
	NH3	0	0.222	/	
Electrolyser power input				15	kW
Electrolyser H_2 outflow				3	Nm^3/h
Cycle inflow molar ratio H_2 to N_2				2.96	-
C-1 and C-2					
Isentropic efficiency				85	%
Mechanical efficiency				100	%
E-1 (internal)					
Temperature approach outlet				10	K
Minimum temperature approach				10	K
Direction of flow			Countercurrent		
R-1, R-2 and R-3					
Type				Plug flow	
Length				0.5	m
Diameter				0.1	m
Catalyst mass				12	kg
Kinetics	Modified Aspen Plus® LLHW kinetics fitted to novel iron-based catalyst data (Koschwitz et al., 2023, 2022b)				
Pressure drop correlation				Ergun	
V-1					
Temperature				15	°C
S-1					
Molar split fraction IX				0.005	-

Table 3 Novel layout exergetic definitions

Component	*Type*	$\dot{E}_Q$ *kJ/hr*	$\dot{E}_W$ *kJ/hr*	$\dot{E}_F$ *kJ/hr*	$\dot{E}_P$ *kJ/hr*	$\dot{E}_L$ *kJ/hr*
M-1	Mixer	/	/	$\dot{E}_{H_2} + \dot{E}_{N_2} + \dot{E}_{XII}$	$\dot{E}_I$	/
C-1	Compressor	/	$P_{el,C-1}$	$P_{el,C-1}$	$\dot{E}_{II} - \dot{E}_I$	/
E-1	Electric heater	/	$P_{el,E-1}$	$P_{el,E-1}$	$\dot{E}_{III} - \dot{E}_I$	/
R-1	Reactor	$\dot{Q}_{Q,R-1}\left(1-\frac{T_0}{T_{R-1}}\right)$	/	$\dot{E}_{III}$	$\dot{E}_{IV} + \dot{E}_{Q,R-1}$	/
R-2	Reactor	$\dot{Q}_{Q,R-2}\left(1-\frac{T_0}{T_{R-2}}\right)$	/	$\dot{E}_{IV}$	$\dot{E}_V + \dot{E}_{Q,R-2}$	/
R-3	Reactor	$\dot{Q}_{Q,R-3}\left(1-\frac{T_0}{T_{R-3}}\right)$	/	$\dot{E}_V$	$\dot{E}_{VI} + \dot{E}_{Q,R-3}$	/
V-1	Vessel	/	$P_{el,V-1}$	$P_{el,V-1} + \dot{E}_{VI} - \dot{E}_{VIII}$	$\dot{E}_{VII}$	/
S-1	Splitter	/	/	$\dot{E}_{VIII}$	$\dot{E}_{IX} + \dot{E}_X$	/
I-1	Valve	/	/	$\dot{E}_{IX} - \dot{E}_X$	/	/
I-2	Valve	/	/	$\dot{E}_{XI} - \dot{E}_{XII}$	/	/
Total		$\sum \dot{E}_Q$	$\sum \dot{E}_W$	$\dot{E}_{H_2} + \dot{E}_{N_2} + \sum \dot{E}_W$	$\dot{E}_{VII}$	$\dot{E}_X + \left\lvert \sum \dot{E}_Q \right\rvert$

Table 4 Conventional layout exergetic definitions

Component	*Type*	$\dot{E}_Q$ *kJ/hr*	$\dot{E}_W$ *kJ/hr*	$\dot{E}_F$ *kJ/hr*	$\dot{E}_P$ *kJ/hr*	$\dot{E}_L$ *kJ/hr*
M-1	Mixer	/	/	$\dot{E}_I + \dot{E}_{XII}$	$\dot{E}_{II}$	/
C-1	Compressor	/	$P_{el,C-1}$	$P_{el,C-1}$	$\dot{E}_{II} - \dot{E}_{H_2} - \dot{E}_{N_2}$	/
E-1	Heat exchanger	/	/	$\dot{E}_{VI} - \dot{E}_{VI-2}$	$\dot{E}_{III} - \dot{E}_{II}$	/
R-1	Reactor	/	$P_{el,R-1}$	$P_{el,R-1} + \dot{E}_{III}$	$\dot{E}_{IV}$	/
R-2	Reactor	$\dot{Q}_{Q,R-2}\left(1-\frac{T_0}{T_{R-2}}\right)$	/	$\dot{E}_{IV}$	$\dot{E}_V + \dot{E}_{Q,R-2}$	/
R-3	Reactor	$\dot{Q}_{Q,R-3}\left(1-\frac{T_0}{T_{R-3}}\right)$	/	$\dot{E}_V$	$\dot{E}_{VI} + \dot{E}_{Q,R-3}$	/
V-1	Vessel	/	$P_{el,V-1}$	$P_{el,V-1} + \dot{E}_{VI-2} - \dot{E}_{VIII}$	$\dot{E}_{VII}$	/
S-1	Splitter	/	/	$\dot{E}_{VIII}$	$\dot{E}_{IX} + \dot{E}_X$	/
I-1	Valve	/	/	$\dot{E}_{IX} - \dot{E}_X$	/	/
C-2	Compressor	/	$P_{el,C-2}$	$P_{el,C-2}$	$\dot{E}_{XII} - \dot{E}_{XI}$	/
Total		$\sum \dot{E}_Q$	$\sum \dot{E}_W$	$\dot{E}_{H_2} + \dot{E}_{N_2} + \sum \dot{E}_W$	$\dot{E}_{VII}$	$\dot{E}_X + \left\lvert \sum \dot{E}_Q \right\rvert$

3.2 Simulation setup

Table 2, Table 3 and Table 4 list the values of the main exergy and Aspen Plus® parameters, the exergetic definitions of the novel and of the conventional cycle components.

In Table 3, the inlet streams of M-1 approximately have the same temperature, which is why the exergetic fuel and product of M-1 are taken to be the actual exergetic in- and outflows of M-1. The components E-1 and V-1 are electrically heated and cooled, for V-1 assuming VCR with a COP of one as a simplified worst case scenario approach. The resulting heat stream of the VCR is neglected. R-1, R-2 and R-3 are electrically heated or cooled, via free convection or if that is insufficient, via ventilated forced air convection, depending on the desired temperature profile in the sections. In the novel layout, the reactors all need to be cooled and give off the heat streams $\dot{Q}_{R-1}$, $\dot{Q}_{R-2}$ and $\dot{Q}_{R-3}$ at temperatures T_{R-1}, T_{R-2} and T_{R-3} to ambient air at T_0. Heat transfer calculations conducted prior to this work suggest that free convection is sufficient. Therefore, the electrical power consumption of the three reactors is zero. I-1 and I-2 are dissipative components for which no exergetic product can be defined. In addition, they serve more the cycle as a whole than other components. Hence, no combined exergetic degree of efficiency with other components can be defined for I-1 and I-2, either. Moreover, by convention, the exergy losses for individual components are set to zero. Lastly, since the exergetic heat streams are all leaving the system and therefore have a negative sign, for the total exergy loss, their absolute value is being used.

In Table 4, unlike R-2 and R-3, R-1 needs to be electrically heated because E-1 cannot supply enough energy to heat up III to the required inlet temperature. Apart from that, the same arguments from above for the novel layout also apply to Table 4 for the conventional layout.

Three main exergetic comparisons of the two P2A cycles were carried out. Their setup and aims are described in detail in the three following Subsections 3.2.1, 3.2.2 and 3.2.3.

3.2.1 EoS comparisons

Several EoS are used in literature to simulate ammonia processes. Bland (2015) uses SRK to model and optimise a conventional methane ammonia synthesis plant. The EoS fits the data provided by the fertiliser company Yara. SRK with no further modifications is also used by Rouwenhorst et al. (2019). RKS-BM with pure NH_3 properties adapted for the synthesis unit and binary interaction parameters for H_2, N_2, Ar and CH_4 adapted to account for the solubilities of these components in NH_3 are used in an Aspen Plus® tutorial (Aspen Tech, 2015). The same EoS is also used for a biomass gasification and ammonia synthesis plant by Arora et al. (2016) and for a green ammonia plant about 30-times smaller than a conventional plant by Lin et al. (2020). Kirova-Yordanova (2004) employs RK and both Tripodi et al. (2018) as well as Adhi and Prasetyo (2018) use PR. In addition, Tripodi et al. (2018) also employ RKS and RKS with modified parameters.

To evaluate how the choice of EoS determines the exergetic results, the five EoS mentioned in the previous paragraph (SRK, RKS-BM, RK, PR and RKS) are compared to the EoS HYSPR-mp. HYSPR-mp is the Aspen HYSYS® Peng Robinson EoS with modified parameters (s. Table 2) which was used in the previous work by Koschwitz

et al. (2022b). It is the aim to determine if the HYSPR-mp is suitable for an exergetic analysis, i.e., gives comparable results to more commonly EoS used in literature.

3.2.2 Chemical exergy comparisons

The chemical exergy is the sum of the ideal chemical exergy and an excess part [s. equation (3)]. The calculation of the excess part [s. equation (4)] is somewhat laborious and is only necessary if the system deviates a lot from being an ideal system.

To evaluate if the system can be regarded as an ideal system, the exergetic indicators with and without the excess part are compared, for both layouts and all six EoS. It is the aim to determine if a time saving ideal exergetic analysis also gives comparable results to an exergy analysis with excess values.

3.2.3 Exergetic analysis

Taking into account the results of the two previous Subsections 3.2.1 and 3.2.2, the two layouts are exergetically evaluated and compared.

The chief aim of this exergy analysis is to determine and compare the overall exergetic degree of efficiency of both cycles. Further, the exergetic weaknesses of the two cycles shall be determined and solutions proposed on how to reduce these irreversibilities, i.e., exergy destructions.

4 Results

The following Sections 4.1, 4.2 and 4.3 correspond to the Subsections 3.2.1, 3.2.2 and 3.2.3.

4.1 Results of the EoS comparisons

The results of the absolute and relative differences in the exergetic stream values of the alternative five EoS to HYSPR-mp are listed in Table 5 and Table 6 for the novel and conventional layout respectively. For better visualisation, Figure 3 depicts the maximum and minimum percentage values of Table 5 and Table 6.

Figure 3 Maximum exergy deviations for all streams and both layouts of the five EoS to HYSPR-mp

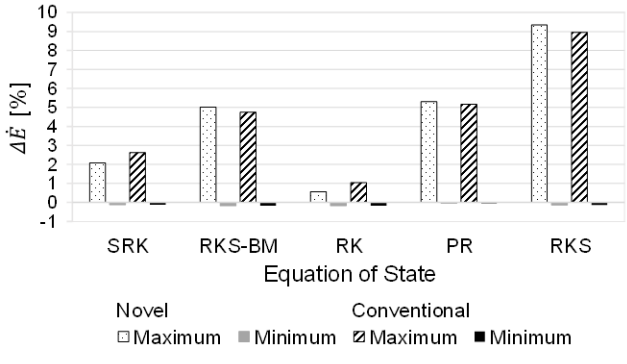

Table 5 Novel layout exergy stream deviations from HYSPR-mp

$\Delta\dot{E}$ [*kJ / hr*]	H_2	N_2	*I*	*II*	*III*	*IV*	*V*	*VI*
SRK	0	0	1,376	1,655	1,779	1,816	1,774	1,756
RKS-BM	–1	0	3,774	3,846	3,927	3,952	3,929	3,918
RK	–1	0	279	455	542	569	541	531
PR	0	0	3,985	4,145	4,224	4,254	4,227	4,214
RKS	–1	0	7,021	7,250	7,381	7,427	7,382	7,359
		VII	*VIII*	*IX*	*X*	*XI*	*XII*	
SRK		–16	1,618	8	8	1,610	1,395	
RKS-BM		–17	3,871	19	19	3,852	3,779	
RK		–5	436	2	2	434	294	
PR		–14	4,139	21	21	4,118	3,992	
RKS		–32	7,254	36	36	7,218	7,030	
$\Delta\dot{E}$ [%]	H_2	N_2	*I*	*II*	*III*	*IV*	*V*	*VI*
SRK	0.0	–0.1	1.3	1.5	1.6	1.6	1.6	1.6
RKS-BM	0.0	–0.2	3.5	3.4	3.5	3.5	3.5	3.6
RK	0.0	–0.2	0.3	0.4	0.5	0.5	0.5	0.5
PR	0.0	0.0	3.7	3.7	3.7	3.8	3.8	3.8
RKS	0.0	–0.1	6.5	6.4	6.5	6.7	6.7	6.7
		VII	*VIII*	*IX*	*X*	*XI*	*XII*	
SRK		–0.1	2.1	2.1	2.1	2.1	1.9	
RKS-BM		–0.1	5.0	5.0	5.0	5.0	5.0	
RK		0.0	0.6	0.6	0.6	0.6	0.4	
PR		0.0	5.3	5.3	5.3	5.3	5.3	
RKS		–0.1	9.3	9.3	9.3	9.3	9.3	

Table 5 and Table 6 reveal that HYSPR-mp calculates lower exergies than the five EoS for the pure streams H_2 and N_2, liquid VII as well as I in the conventional layout. The absolute and percentage exergy differences are negative but rather small, i.e., not below –0.2%. This can be explained by the fact that in all these streams one component is dominant, such that they can be regarded as almost pure streams or, in the case of stream I, by the lack of NH_3. For the other streams for both layouts, HYSPR-mp leads to higher exergies than the five EoS, i.e., the absolute and percentage exergy differences are positive. For these streams, RK displays the smallest and RKS the biggest percentage differences. SRK is second closest to HYSPR-mp with an average deviation of ca. 2%, whereas RKS-BM and PR both deviate by ca. 3.4%–5.3%.

Judging from Table 5, Table 6 and Figure 3, with a maximum of 9.3% for RKS and a minimum stream exergy deviation of –0.2% for RK, it can be claimed that all EoS are within a reasonable range of one another and ergo the results of HYSPR-mp should be reasonable.

The results of the exergetic indicators for the novel and conventional layout are listed in Table 7 and Table 8. For better visualisation, Figure 4 depicts the maximum and minimum percentage values of Table 7 and Table 8.

Table 6 Conventional layout exergy stream deviations from HYSPR-mp

$\Delta\dot{E}$ [*kJ / hr*]	H_2	N_2	*I*	*II*	*III*	*IV*	*V*	*VI*
SRK	0	0	–5	1,978	2,036	2,228	2,198	2,168
RKS-BM	–1	0	–10	3,639	3,664	3,756	3,736	3,722
RK	–1	0	–10	771	811	945	926	907
PR	0	0	–3	3,960	3,993	4,113	4,090	4,072
RKS	0	0	–5	1,978	2,036	2,228	2,198	2,168
	VI-2	*VII*	*VIII*	*IX*	*X*	*XI*	*XII*	
SRK	2,053	–18	2,026	10	10	2,016	2,018	
RKS-BM	3,675	–16	3,677	18	18	3,659	3,659	
RK	829	–7	808	4	4	804	805	
PR	4,007	–13	3,999	20	20	3,979	3,980	
RKS	6,951	–30	6,948	35	35	6,913	6,915	
$\Delta\dot{E}$ [%]	H_2	N_2	*I*	*II*	*III*	*IV*	*V*	*VI*
SRK	0.0	–0.1	0.0	1.8	1.8	2.0	2.0	2.0
RKS-BM	0.0	–0.2	0.0	3.3	3.3	3.4	3.4	3.4
RK	0.0	–0.2	0.0	0.7	0.7	0.9	0.8	0.8
PR	0.0	0.0	0.0	3.6	3.6	3.7	3.7	3.7
RKS	0.0	–0.1	0.0	6.2	6.2	6.4	6.4	6.4
	VI-2	*VII*	*VIII*	*IX*	*X*	*XI*	*XII*	
SRK	1.9	–0.1	2.6	2.6	2.6	2.6	2.6	
RKS-BM	3.4	–0.1	4.7	4.7	4.7	4.7	4.7	
RK	0.8	0.0	1.0	1.0	1.0	1.0	1.0	
PR	3.7	0.0	5.2	5.2	5.2	5.2	5.2	
RKS	6.4	–0.1	9.0	9.0	9.0	9.0	9.0	

Table 7 Novel layout exergetic results deviations from HYSPR-mp

	$\dot{E}_D$		$\Delta\epsilon$		$\Delta\xi$	
	kJ/hr	*%*	*%.*	*%*	*%.*	*%*
SRK	1,023.8	7.5	–1.5	–2.3	1.6	5.4
RKS-BM	425.7	3.1	–0.6	–1.0	0.6	2.2
RK	669.0	4.9	–1.0	–1.5	1.0	3.5
PR	619.9	4.6	–0.9	–1.4	0.9	3.3
RKS	931.5	6.8	–1.4	–2.2	1.4	4.9

Table 8 Conventional layout exergetic results deviations from HYSPR-mp

	$\dot{E}_D$		$\Delta\epsilon$		$\Delta\xi$	
	kJ/hr	*%*	*%.*	*%*	*%.*	*%*
SRK	1,087.3	9.0	–1.9	–2.7	1.8	6.6
RKS-BM	424.8	3.5	–0.8	–1.1	0.7	2.5
RK	728.0	6.0	–1.2	–1.8	1.2	4.4
PR	628.5	5.2	–1.1	–1.6	1.0	3.8
RKS	933.9	7.7	–1.7	–2.4	1.5	5.6

Figure 4 Maximum exergetic indicator deviations for both layouts of the five EoS to HYSPR-mp

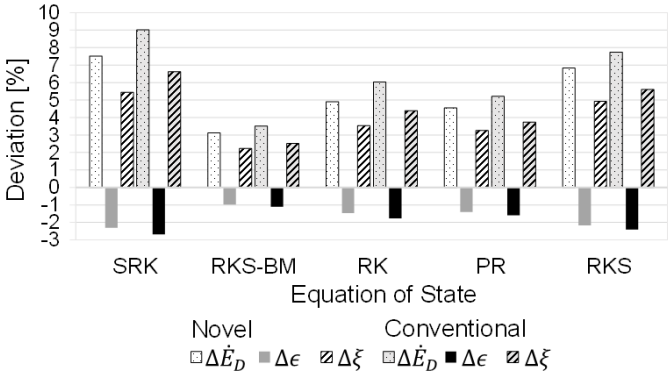

The data in Table 7 and Table 8 reveals that HYSPR-mp overestimates $\dot{E}_D$ and ξ but underestimates ϵ. This suggests that HYSPR-mp yields rather conservative exergetic indicator values. From Figure 4, it can be seen that the differences for all five other EoS and both layouts are in between the values of SRK, i.e., below the maximum of 9.0% for $\Delta\dot{E}_D$, above the minimum –2.7% for $\Delta\epsilon$ and below the maximum 6.6% for $\Delta\xi$. This suggests as well that HYSPR-mp yields reasonable exergetic results. Overall for the exergetic indicators, SRK and RKS deviate the most, RK and PR are in between and RKS-BM deviates the least from HYSPR-mp.

Summarising, for all of the five EoS (SRK, RKS-BM, RK, PR and RKS) compared to HYSPR-mp, the maximum percentage difference is within ±10% for the exergy streams (s. Figure 3) as well as for the exergetic indicators (s. Figure 4). Therefore, it can be assumed that HYSPR-mp likely gives reasonable and reliable results that are within range of those five other EoS used in literature to simulate ammonia processes. This also means that HYSPR-mp can be used for the exergy analysis in Section 4.3 as well as for the upcoming exergy costing comparison of the two cycles.

4.2 Results of the chemical exergy comparisons

The comparisons of the chemical exergies revealed that the differences of real to ideal (index id) chemical exergies are marginal. This is true for the stream exergies as well as the exergetic indicators for both layouts. Analogously to Figure 3, Figure 5 depicts the maximum and minimum percentage stream exergies for both layouts and all streams. The

maximum and minimum percentage differences are 0.0008 for RKS and close to –0.006% for all EoS.

Figure 5 Maximum real to ideal exergy deviations of the six EoS for all streams and both layouts

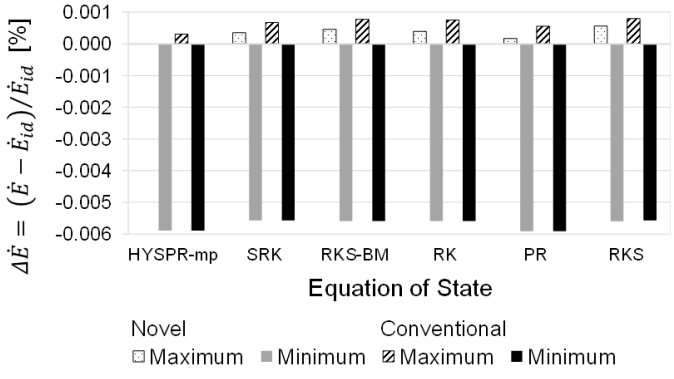

Analogously to Figure 4, Figure 6 depicts the maximum and minimum exergetic indicator real to ideal percentage differences for both layouts. The maximum percentage difference is 0.0159% for $\Delta\dot{E}_D$ and $\Delta\xi$ and the minimum is –0.00591% for $\Delta\epsilon$ (all for PR). The real exergies overestimate $\dot{E}_D$ and ξ, but underestimate ϵ. This means that the real exergies produce more conservative values. This is true for all EoS and both layouts.

Summarising, the results of the chemical exergy comparisons show that the excess values have a marginal impact on the (chemical) exergies. Thus, it can be argued that the excess values can be neglected, saving programming and calculation time without significantly affecting the accuracy of the exergetic evaluation. This further means that a reduced chemical exergy analysis suffices for the exergy analysis in Section 4.3 as well as for the upcoming exergy costing comparison of the two cycles.

Figure 6 Maximum real to ideal exergetic indicator deviations of the six EoS for both layouts

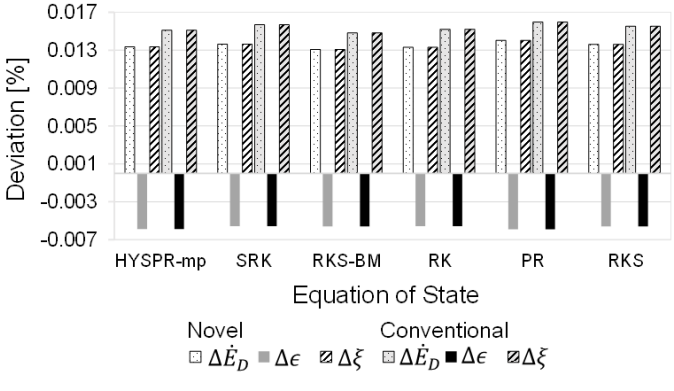

4.3 Results of the exergetic analysis

Taking the results from the previous Sections 4.1 and 4.2, HYSPR-mp with ideal chemical exergies is being employed in this section. However, as a first step in order to fairly compare the two cycles, both cycles need to operate at their optimal reactor temperature profile. As determined by Koschwitz et al. (2022b), for the novel layout this profile is 380°C, 380°C, 350°C and 340°C for the outlet temperature of the electrical preheater and the temperatures in R-1, R-2 and R-3. However, this profile may not be optimal for the conventional layout. Thus, a variation analysis for the conventional layout for the three reactor temperatures from 350°C to 410°C, 320°C to 380°C and 310°C to 370°C, a sensible range of ± 30 K in steps of 10 K, was carried out, to determine the optimal profile with regards to a maximum total exergetic efficiency.

The result of the variation analysis is depicted in Figure 7. The optimal reactor temperature profile is 380°C, 360°C and 340°C for a maximum total exergetic value of 69.47%. Compared to the novel profile, only T_{R-2} increases from 350°C to 360°C. From a kinetic and thermodynamic point of view, the result of the variation analysis makes sense, as the expected falling reactor temperature profile is maintained and only slightly changed.

Figure 7 Optimum (black column) reactor temperature profile variation analysis result (ϵ_{tot} = 69.47%; T_{R-1}, T_{R-2}, T_{R-3} = 380°C, 360°C, 340°C) for the conventional layout

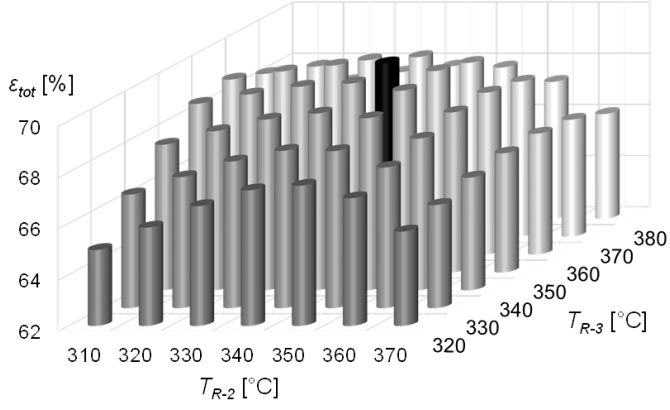

With this optimal profile, the exergetic analysis is carried out. The stream variable results of the novel and conventional layout are given in Table 9 and Table 10. The results of the exergetic analysis are given in Table 11 and Table 12.

Comparing Table 9 and Table 10, it first strikes out that the stream values of the output VII as well as the recycle XII and the purge XI are almost the same, at least to the number of decimal places given in the tables. This means that both layouts have not only the same input, but also similar outlets as well as internal streams.

What differs is the energy needed for heating the reactor, which is smaller in the novel than in the conventional layout and is shifted from the preheater to the electrical heater of the first reactor section, i.e., $P_{el,E-1}$ = 1,591 kJ/h in Table 9 vs. $P_{el,R-1}$ = 2,282 kJ/h in Table 10. This suggests that E-1 (internal) cannot transfer all the energy needed to heat up the reactor inflow. The reason for this is the lower inlet temperature of II into E-1 (internal). This, in turn, can be explained by the fact that in the novel layout the complete

recycle enters C-1, resulting in an already well-heated outlet stream. Therefore, the question arises whether the internal heat exchanger in the conventional layout really poses that much of a benefit, given that in the novel layout C-1 already acts as a sort of heater and E-1 (electric) only needs to raise the temperature by ca. 80 K.

Table 9 Novel layout stream variable results

Stream		H_2	N_2	*I*	*II*	*III*	*IV*	*V*	*VI*
$\dot{M}$	kg/hr	0.27	1.27	7.94	7.94	7.94	7.94	7.94	7.94
$\dot{N}$	kmol/hr	0.13	0.05	0.64	0.64	0.64	0.58	0.56	0.55
T	°C	20.00	20.00	7.58	301.44	380.00	380.00	350.00	340.00
p	bar	9.01	9.01	9.01	81.01	81.01	81.01	81.01	81.01
y_{H_2}	mol/mol	1.00	0.00	0.56	0.56	0.56	0.46	0.43	0.41
y_{N_2}	mol/mol	0.00	1.00	0.34	0.34	0.34	0.33	0.32	0.32
y_{NH_3}	mol/mol	0.00	0.00	0.09	0.09	0.09	0.21	0.24	0.27
$\overline{e}^{PH}$	kJ/kmol	5426	5411	5431	13,377	14,650	14,794	14,281	14,118
$\overline{e}^{CH}$	kJ/kmol	236,100	720	162,032	162,032	162,032	177,577	182,219	185,124
$\dot{E}$	kJ/hr	32,328	277	107,489	112,589	113,406	111,479	110,693	110,317
			VII	*VIII*	*IX*	*X*	*XI*	*XII*	
$\dot{M}$	kg/hr		1.50	6.43	0.03	0.03	6.40	6.40	
$\dot{N}$	kmol/hr		0.09	0.47	0.00	0.00	0.46	0.46	
T	°C		15.00	15.00	15.00	15.00	15.00	3.11	
p	bar		79.01	79.01	79.01	79.01	79.01	9.01	
y_{H_2}	mol/mol		0.00	0.49	0.49	0.49	0.49	0.49	
y_{N_2}	mol/mol		0.00	0.38	0.38	0.38	0.38	0.38	
y_{NH_3}	mol/mol		0.99	0.13	0.13	0.13	0.13	0.13	
$\overline{e}^{PH}$	kJ/kmol		5,831	10,761	10,761	10,761	10,761	5,437	
$\overline{e}^{CH}$	kJ/kmol		342,406	157,073	157,073	157,073	157,073	157,073	
$\dot{E}$	kJ/hr		30,841	78,063	390	390	77672	75,209	
		$P_{el,C-1}$	$P_{el,E-1}$	$P_{el,R-1}$	$P_{el,R-2}$	$P_{el,R-3}$	$P_{el,V-1}$		
$\dot{E}_W$	kJ/hr	5,726	1,591	/	/	/	7,825		

However, the fact that the whole recycle is being compressed results in a much higher electrical power demand of compression in the novel layout, i.e., $P_{el,C-1}$ = 5,726 kJ/h in Table 9 vs. $P_{el,C-1} + P_{el,C-2}$ = 1,719 kJ/h in Table 10.

The last value that strikes out is the similar cooling requirement in the condenser $P_{el,V-1}$, which is only slightly higher for the novel layout, i.e., 7,825 kJ/h in Table 9 vs. 7,797 kJ/h in Table 10. One would expect, given the higher temperature in the novel layout, i.e., 340 of VI in Table 9 vs. 223.14°C of VI-2 in Table 10, but besides that almost identical stream properties, that the condensing energy required in the novel

layout would be much higher. However, the condensation of NH_3 is much more energy intensive than the cooling of the stream. This results in an almost similar energy uptake in V-1 in both layouts.

Table 10 Conventional layout stream variable results

Stream		*H_2*	*N_2*	*I*	*II*	*III*	*IV*	*V*	*VI*
$\dot{M}$	kg/hr	0.27	1.27	1.54	7.91	7.91	7.91	7.91	7.91
$\dot{N}$	kmol/hr	0.13	0.05	0.18	0.64	0.64	0.58	0.56	0.55
T	°C	20.00	20.00	338.55	102.11	213.14	380.00	360.00	340.00
p	bar	9.01	9.01	81.01	81.01	81.01	81.01	81.01	81.01
y_{H_2}	mol/mol	1.00	0.00	0.75	0.56	0.56	0.46	0.43	0.41
y_{N_2}	mol/mol	0.00	1.00	0.25	0.35	0.35	0.33	0.32	0.32
y_{NH_3}	mol/mol	0.00	0.00	0.00	0.09	0.09	0.21	0.25	0.27
$\overline{e}^{PH}$	kJ/kmol	5,426	5,411	13,867	11,117	12,170	14,794	14,463	14,118
$\overline{e}^{CH}$	kJ/kmol	236,100	720	175,260	161,925	161,925	177,496	182,234	185,115
$\dot{E}$	kJ/hr	32,328	277	33,867	110,605	111,278	110,940	110,250	109,776
		VI-2	*VII*	*VIII*	*IX*	*X*	*XI*	*XII*	
$\dot{M}$	kg/hr	7.91	1.50	6.40	0.03	0.03	6.37	6.37	
$\dot{N}$	kmol/hr	0.55	0.09	0.46	0.00	0.00	0.46	0.46	
T	°C	223.14	15.00	15.00	15.00	15.00	15.00	17.54	
p	bar	79.01	79.01	79.01	79.01	79.01	79.01	81.01	
y_{H_2}	mol/mol	0.41	0.00	0.49	0.49	0.49	0.49	0.49	
y_{N_2}	mol/mol	0.32	0.00	0.38	0.38	0.38	0.38	0.38	
y_{NH_3}	mol/mol	0.27	0.99	0.13	0.13	0.13	0.13	0.13	
$\overline{e}^{PH}$	kJ/kmol	12,204	5,831	10,761	10,761	10,761	10,761	10,820	
$\overline{e}^{CH}$	kJ/kmol	185,115	342,404	156,896	156,896	156,896	156,896	156,896	
$\dot{E}$	kJ/hr	108,721	30,844	77,528	388	388	77,140	77,167	
		$P_{el,C-1}$		$P_{el,R-1}$	$P_{el,R-2}$	$P_{el,R-3}$	$P_{el,V-1}$	$P_{el,C-2}$	
$\dot{E}_W$	kJ/hr	1,685		2,282	/	/	7,797	34	

Looking at the exergetic values of the two processes in Table 11 and Table 12, the first thing that catches the eye is that the reactor cooling in the novel layout is almost thrice that of the conventional layout and thus the exergy of heat unused and lost is almost three times as high, i.e., $\dot{E}_{Q,tot} = -2,900$ kJ/h in Table 11 vs. –1,121 kJ/h in Table 12. Thus, together with the purge X leaving the cycle, the exergetic losses in the novel cycle are almost double, i.e., $\dot{E}_{L,tot} = 3,290$ kJ/h in Table 11 vs. 1,509 kJ/h in Table 12. Also, the novel cycle has a higher exergetic fuel demand, i.e., $\dot{E}_{F,tot} = 47,747$ kJ/h in Table 11 vs. 44,404 kJ/h in Table 12. This can be attributed to the higher demand for exergetic power,

i.e., $\dot{E}_{W,tot} = 15{,}142$ kJ/h in Table 11 vs. 11,799 kJ/h in Table 12. At the same time, with VII being almost identical in both layouts, the exergetic product of both cycles is almost identical. This results in a lower total exergetic efficiency in the novel layout with a difference of 4.87%., i.e., $\epsilon_{tot} = 64.59\%$ in Table 11 vs. 69.46% in Table 12.

Perhaps not surprisingly, in the novel layout in Table 11 the recycle valve I-2 displays the lowest exergetic efficiency ($\epsilon_{I-2} = 0\%$) as well as both the second highest exergetic ratio of destruction to feed ($\xi_{I-2} = 5.16\%$) and exergetic destruction ratio ($\phi_{I-2} = 18.09\%$). However, the biggest share in exergy destruction is caused in V-1 with values of $\epsilon_{V-1} = 76.95\%$, $\xi_{V-1} = 19.35\%$ and $\phi_{V-1} = 67.84\%$. This means that the cooling of the reactor outlet causes by far the greatest irreversibilities. This suggests that a different separation method, e.g., ad- or absorption at a higher temperature, as put forward in Palys et al. (2018), Malmali et al. (2018) or Smith et al. (2019), might be exergetically beneficial. However, these methods make the cycle operation more complicated, i.e., by the batch-wise removal of NH_3 and the recycling of the adsorption bed or absorption material.

In the conventional cycle in Table 12, V-1 displays a similar dominance on the exergetic performance, followed by R-1 with $\dot{E}_{D,R-1} = 2{,}620$ kJ/h, $\xi_{R-1} = 5.90\%$ and $\phi_{R-1} = 21.74\%$. This can be explained again by the fact that E-1 (internal) does not preheat the reactor inlet as much as the combination of C-1 and E-1 (electric) in the novel layout. The resulting temperature difference has to be bridged by the electrical heating in R-1, resulting in irreversibilities and a low exergetic performance of R-1.

Summarising, the results of the exergetic analysis show that the novel layout only has a 4.87 percentage point lower exergetic degree of efficiency, with a value of 64.59% compared to 69.46% of the conventional layout. This rather small difference is remarkable, given that the novel layout is much simpler. Furthermore, the integral part of the conventional cycle, the internal heat exchanger, does not seem to be that beneficial, as it cannot provide all the energy needed for heating up the reactor inlets. This in turn leads to a high exergy destruction in the first reactor compartment due to the required electrical heat-up there.

On the contrary, in the novel layout the heating up is already partly done during the compression in the compressor. The compressor in the novel cycle displays the main exergetic uptake. Therefore, its efficiency should be improved. This can be achieved by choosing a high-end compressor. Since the novel cycle employs only one instead of two compressors, a larger investment in a high-end compressor is likely to be less costly than the investment cost of two less efficient compressors for the conventional cycle. However, such trade-off calculations will be made and discussed extensively in the upcoming exergy costing analysis of the two cycles, for which this exergy analysis has laid the foundation.

The main exergetic losses in the novel layout are related to the heat losses in the three reactor sections. However, these heat losses have to be accepted as part of the novel cycle design. The same is true for the high exergy destruction in the recycle valve. In both layouts, the highest share of exergy destruction is caused by the condenser. To reduce the irreversibilities there, a different way of removing the ammonia from the cycle at higher temperatures might be a solution, e.g., via ad- or absorption. However, this would lead to a more complicated design and operation of the cycle and possibly also to higher investment costs.

Table 11 Novel layout exergetic results

Component	*Type*	$\dot{E}_Q$ *kJ/hr*	$\dot{E}_W$ *kJ/hr*	$\dot{E}_F$ *kJ/hr*	$\dot{E}_P$ *kJ/hr*	$\dot{E}_L$ *kJ/hr*	$\dot{E}_D$ *kJ/hr*	ϵ *%*	ξ *%*	ϕ *%*
M-1	Mixer	/	/	107,814	107,489	/	326	99.70	0.68	2.39
C-1	Compressor	/	5,726	5,726	5,100	/	626	89.07	1.31	4.60
E-1	Electric heater	/	1,591	1,591	817	/	774	51.36	1.62	5.68
R-1	Reactor	–1,789	/	113,406	113,268	/	138	99.88	0.29	1.02
R-2	Reactor	–751	/	111,479	111,444	/	35	99.97	0.07	0.25
R-3	Reactor	–360	/	110,693	110,677	/	17	99.98	0.03	0.12
V-1	Vessel	/	7,825	40,079	30,841	/	9,238	76.95	19.35	67.84
S-1	Splitter	/	/	78,063	78,063	/	0	100.00	0.00	0.00
I-1	Valve	/	/	0	0	/	0	0.00	0.00	0.00
I-2	Valve	/	/	2,464	0	/	2,464	0.00	5.16	18.09
Total		–2,900	15,142	47,747	30,841	3,290	13,616	64.59	28.52	/

Table 12 Conventional layout exergetic results

Component	*Type*	$\dot{E}_Q$	$\dot{E}_W$	$\dot{E}_F$	$\dot{E}_P$	$\dot{E}_L$	$\dot{E}_D$	ϵ	ξ	ϕ
		kJ/hr	*kJ/hr*	*kJ/hr*	*kJ/hr*	*kJ/hr*	*kJ/hr*	%	%	%
M-1	Mixer	/	/	111,034	110,605	/	429	99.61	0.97	3.56
C-1	Compressor	/	1,685	1,685	1,262	/	424	74.85	0.95	3.52
E-1	Heat exchanger	/	/	1,055	673	/	382	63.80	0.86	3.17
R-1	Reactor	/	2,282	113,560	110,940	/	2,620	97.69	5.90	21.74
R-2	Reactor	–666	/	110,940	110,916	/	25	99.98	0.06	0.21
R-3	Reactor	–455	/	110,250	110,231	/	18	99.98	0.04	0.15
V-1	Vessel	/	7,797	38,990	30,844	/	8,147	79.11	18.35	67.60
S-1	Splitter	/	/	77,528	77,528	/	0	100.00	0.00	0.00
I-1	Valve	/	/	0	0	/	0	0.00	0.00	0.00
C-2	Compressor	/	34	34	27	/	7	79.55	0.02	0.06
Total		-1121	11,799	44,404	30,844	1,509	12,052	69.46	27.14	/

5 Conclusions

In this work an exergetic comparison between a novel and a conventional small-scale P2A system has been carried out. The analysis is split into three parts. First, five EoS commonly found in ammonia process simulation literature are compared to the EoS HYSPR-mp previously introduced in Koschwitz et al. (2022b) to determine if HYSPR-mp is a suitable EoS. Second, the two systems are evaluated by using both an extended and ideal calculation of chemical exergies, i.e., with and without excess values. This is done to determine if an ideal exergy analysis describes the systems adequately and thus calculation and programming time for the excess values can be saved. Third, building on the results of the first two parts, the exergetic comparison of the two P2A systems is carried out.

The EoS comparison shows that the maximum percentage difference of HYSPR-mp to the five EoS (SRK, RKS-BM, RK, PR and RKS) is within ±10% for the exergy streams as well as for the exergetic indicators. Therefore, HYSPR-mp seems to be a suitable EoS for the exergy comparison.

The chemical exergy comparison shows that the excess values have a marginal impact on the (chemical) exergies. The real to ideal exergetic stream and indicator differences for both layouts and all streams lie within ±0.02%. Thus, it can be argued that the excess values can be neglected, saving programming and calculation time, whilst keeping the exergy evaluation accurate.

Taking the results of the EoS and chemical exergy comparison into consideration, for the exergetic comparison of the two P2A systems HYSPR-mp with ideal chemical exergies is used. The results of this comparison show that the novel layout only has a 4.87 percentage point lower exergetic degree of efficiency with a value of 64.59% compared to 69.46% of the conventional layout. Thus, the novel layout is slightly exergetically inferior to the conventional design. The novel design possesses process-inherent exergy destruction in the pressure reducing recycle valve as well as exergy lost due to the unused thermal exergy of the reactor outlet stream. However, an upcoming exergy costing analysis, for which the exergetic analysis in this work is the basis, will show that these exergy inefficiencies will be compensated by the lower investment cost of the novel cycle, as the recycle valve and the electrical heater in the novel design are less costly than the recycle compressor and the internal gas-gas heat exchanger in the conventional design.

Looking ahead, the thorough exergetic study of this work will be the basis for first an exergy costing and later an exergy environmental evaluation of the two layouts. The exergy costing study will reveal that the lower exergetic degree of efficiency of the novel layout can be compensated by its lower investment cost. The exergy environmental study will reveal how the novel layout compares to the conventional layout in terms of its impact on the environment. After all, future storage systems of renewable energies should not only be economical, but also ecological.

Acknowledgements

This project has received funding from the European Union's Horizon 2020 research and innovation programme under Grant Agreement No. 884157. https://flexnconfu.eu/. (see online version for colours)

Pascal Koschwitz contributed to conceptualisation, methodology and writing – original draft. Daria Bellotti contributed to project administration and writing – review and editing. Cheng Liang contributed to writing – review and editing. Bernd Epple contributed to funding acquisition.

References

Adhi, T.P. and Prasetyo, M.I. (2018) 'Process stability identification through dynamic study of single-bed ammonia reactor with feed-effluent heat exchanger (FEHE)', *MATEC Web of Conferences*, Vol. 156, p.3003, https://doi.org/10.1051/matecconf/201815603003.

Allman, A. and Daoutidis, P. (2018) 'Optimal scheduling for wind-powered ammonia generation: effects of key design parameters', *Chemical Engineering Research and Design*, Vol. 131, pp.5–15, https://doi.org/10.1016/j.cherd.2017.10.010.

Appl, M. (2000a) 'Ammonia, 1. Introduction', in *Ullmann's Encyclopedia of Industrial Chemistry*, Wiley-VCH Verlag GmbH & Co. KGaA, Weinheim, Germany.

Appl, M. (2000b) 'Ammonia, 2. Production processes', in *Ullmann's Encyclopedia of Industrial Chemistry*, Wiley-VCH Verlag GmbH & Co. KGaA, Weinheim, Germany.

Appl, M. (2000c) 'Ammonia, 3. Production plants', in *Ullmann's Encyclopedia of Industrial Chemistry*, Wiley-VCH Verlag GmbH & Co. KGaA, Weinheim, Germany.

Araújo, A and Skogestad, S (2008) 'Control structure design for the ammonia synthesis process', *Computers & Chemical Engineering*, Vol. 32, No. 12, pp.2920–2932, https://doi.org/10.1016/j.compchemeng.2008.03.001.

Arora, P., Hoadley, A.F.A., Mahajani, S.M. and Ganesh, A. (2016) 'Small-scale ammonia production from biomass: a techno-enviro-economic perspective', *Industrial & Engineering Chemistry Research*, Vol. 55, No. 22, pp.6422–6434, https://doi.org/10.1021/acs.iecr.5b04937.

Aspen Tech (2015) *Aspen Plus Ammonia Model* [online] https://user.eng.umd.edu/~nsw/chbe446/Ammonia-Aspen.pdf (accessed 5 December 2022).

Aspen Tech (2023) *Aspen Plus. Version V11 (37.0.0.395)* [online] https://www.aspentech.com/en/products/engineering/aspen-plus (accessed 21 February 2023).

Bañares-Alcántara, R., Dericks III, G., Fiaschetti, M., Grünewald, P., Lopez, J.M, Tsang, E., Yang, A., Ye, L. and Zhao, S. (2015) *Analysis of Islanded Ammonia-Based Energy Storage Systems*, University of Oxford, Oxford.

Bazzanella, A.M., Ausfelder, F. and DECHEMA Gesellschaft für Chemische Technik und Biotechnologie e.V. (2017) *Low Carbon Energy and Feedstock for the European Chemical Industry*, Technology Study, Frankfurt am Main, DECHEMA e.V.

Bejan, A., Tsatsaronis, G. and Moran, M.J. (1996) *Thermal Design and Optimization*, Wiley, New York.

Bland, M.J. (2015) *Optimisation of an Ammonia Synthesis Loop*, Norwegian University of Science and Technology, Trondheim.

Bothinah, A., Gary, M. and Martin, E.B. (2016) 'Dynamic process monitoring of an ammonia synthesis fixed-bed reactor', *International Journal of Mechanical and Mechatronics Engineering*, Vol. 10, No. 3, pp.462–472, https://doi.org/10.5281/zenodo.1111691.

Bram, S. and Ruyck, J.D. (1997) 'Exergy analysis tools for Aspen applied to evaporative cycle design', *Energy Conversion and Management*, Vol. 38, Nos. 15–17, pp.1613–1624, https://doi.org/10.1016/S0196-8904(96)00222-1.

Brown, T. (2020) *Green Ammonia at Oil and Gas Scale: the 15 GW Asian Renewable Energy Hub* [online] https://www.ammoniaenergy.org/articles/green-ammonia-at-oil-and-gas-scale-the-15-gw-asian-renewable-energy-hub/ (accessed 5 December 2022).

Elishav, O., Mosevitzky Lis, B., Miller, E.M., Arent, D.J., Valera-Medina, A., Grinberg Dana, A., Shter, G.E. and Grader, G.S. (2020) 'Progress and prospective of nitrogen-based alternative fuels', *Chemical Reviews*, Vol. 120, No. 12, pp.5352–5436, https://doi.org/10.1021/acs.chemrev.9b00538.

Gupta, A., Anand, Y., Anand, S. and Tyagi, S.K. (2015) 'Thermodynamic optimization and chemical exergy quantification for absorption-based refrigeration system', *Journal of Thermal Analysis and Calorimetry*, Vol. 122, No. 2, pp.893–905, https://doi.org/10.1007/s10973-015-4795-6.

Inamuddin, Boddula, R. and Asiri, AM. (2020) *Sustainable Ammonia Production*, Springer International Publishing, Cham.

Jacobsen, D. (2020) 'A marine fuel standard for ammonia – an engine designers perspective', *Conference Talk at the 2020 Ammonia Energy Association Conference* [online] https://www.ammoniaenergy.org/wp-content/uploads/2020/12/Dorthe-Jacobsen.pdf (accessed 1 December 2022).

Jinasena, A., Bernt, L. and Bjørn, G. (2018) 'Dynamic model of an ammonia synthesis reactor based on open information', in *Proceedings of The 9th EUROSIM Congress on Modelling and Simulation, EUROSIM 2016, The 57th SIMS Conference on Simulation and Modelling SIMS 2016, Proceedings of The 9th EUROSIM Congress on Modelling and Simulation, EUROSIM 2016, The 57th SIMS Conference on Simulation and Modelling SIMS 2016*, Linköping, Linköping University Electronic Press, 12–16 September, pp.998–1004.

Kasiri, N., Hosseini, A.R. and Moghadam, M. (2003) 'Dynamic simulation of an ammonia synthesis reacto', in *European Symposium on Computer Aided Process Engineering-13, 36th European Symposium of the Working Party on Computer Aided Process Engineering*, Amsterdam, Elsevier, pp.695–700.

Kirova-Yordanova, Z. (2004) 'Exergy analysis of industrial ammonia synthesis', *Energy*, Vol. 29, Nos. 12–15, pp.2373–2384, https://doi.org/10.1016/j.energy.2004.03.036.

Kobayashi, H. (2014) *Power Generation by Combustion using Ammonia* [online] https://www.jst.go.jp/EN/achievements/research/bt111-112.html (accessed 5 December 2022).

Koschwitz, P., Bellotti, D., Liang, C. and Epple, B. (2022a) 'Dynamic simulation of a novel small-scale power to ammonia concept', *Energy Proceedings Volume 28: Closing Carbon Cycles – A Transformation Process Involving Technology, Economy, and Society: Part III*, ISSN: 2004-2965, https://doi.org/10.46855/energy-proceedings-10247.

Koschwitz, P., Bellotti, D., Liang, C. and Epple, B. (2022b) 'Steady state process simulations of a novel containerized power to ammonia concept', *International Journal of Hydrogen Energy*, Vol. 4, No. 60, pp.25322–25334, https://doi.org/10.1016/j.ijhydene.2022.05.288.

Koschwitz, P., Bellotti, D., Sanz, M.C., Alcaide-Moreno, A., Liang, C. and Epple, B. (2023) 'Dynamic parameter simulations for a novel small-scale power-to-ammonia concept', *Processes*, Vol. 11, No. 3, p.680, https://doi.org/10.3390/pr11030680.

Lazzaretto, A. and Tsatsaronis, G. (2006) 'SPECO: a systematic and general methodology for calculating efficiencies and costs in thermal systems', *Energy*, Vol. 31, Nos. 8–9, pp.1257–1289, https://doi.org/10.1016/j.energy.2005.03.011.

Lin, B., Wiesner, T. and Malmali, M. (2020) 'Performance of a small-scale Haber process: a techno-economic analysis', *ACS Sustainable Chemistry & Engineering*, Vol. 8, No. 41, pp.15517–15531, https://doi.org/10.1021/acssuschemeng.0c04313.

Malmali, M., Le, G., Hendrickson, J. and Prince, J., McCormick, A.V. and Cussler, E.L. (2018) 'Better absorbents for ammonia separation', *ACS Sustainable Chemistry & Engineering*, Vol. 6, No. 5, pp.6536–6546, https://doi.org/10.1021/acssuschemeng.7b04684.

Meyer, L. (Ed.) (2006) *Exergiebasierte Untersuchung der Entstehung von Umweltbelastungen in Energieumwandlungsprozessen auf Komponentenebene, Exergoökologische Analyse*, Darmstadt, Techn. Zugl., Univ., Diss., Darmstadt, Inst. WAR.

Meyer, L., Tsatsaronis, G., Buchgeister, J. and Schebek, L. (2009) 'Exergoenvironmental analysis for evaluation of the environmental impact of energy conversion systems', *Energy* , Vol. 4, No. 1, pp.75–89, https://doi.org/10.1016/j.energy.2008.07.018.

Moran, M.J., Shapiro, H.N., Boettner, D.D. and Bailey, M.B. (2014) *Fundamentals of Engineering Thermodynamics*, Wiley, Hoboken, N.J.

Morlanés, N., Katikaneni, Sai, P., Paglieri, S.N., Harale, A., Solami, B., Sarathy, S.M. and Gascon, J. (2021) 'A technological roadmap to the ammonia energy economy: Current state and missing technologies', *Chemical Engineering Journal*, Vol. 408, 127310, https://doi.org/10.1016/j.cej.2020.127310.

Morud, J.C. and Skogestad, S. (1998) 'Analysis of instability in an industrial ammonia reactor', *AIChE Journal*, Vol. 44, No. 4, pp.888–895, https://doi.org/10.1002/aic.690440414.

Osuolale, F.N. and Zhang, J. (2018) 'Exergetic optimisation of atmospheric and vacuum distillation system based on bootstrap aggregated neural network models', in Fethi, A. and Dincer, I. (Eds.): *Exergy for A Better Environment and Improved Sustainability 1,* pp.1033–1046, Springer International Publishing, Cham, Switzerland.

Palys, M., McCormick, A., Cussler, E. and Daoutidis, P. (2018) 'Modeling and optimal design of absorbent enhanced ammonia synthesis', *Processes*, Vol. 6, No. 7, p.91, https://doi.org/10.3390/pr6070091.

Patil, B.S., Hessel, V., Seefeldt, L.C., Dean, D.R., Hoffman, B.M., Cook, B.J. and Murray, L.J. (2000) 'Nitrogen fixation', in *Ullmann's Encyclopedia of Industrial Chemistry*, pp.1–21, Wiley-VCH Verlag GmbH & Co. KGaA, Weinheim, Germany.

Penkuhn, M. and Tsatsaronis, G. (2017) 'Comparison of different ammonia synthesis loop configurations with the aid of advanced exergy analysis', *Energy*, Vol. 137, pp.854–864, https://doi.org/10.1016/j.energy.2017.02.175.

Radgen, P. and Lucas, K. (1996) Energy system analysis is fertilizer complex – pinch analysis vs. Exergy analysis. *Chemical Engineering & Technology*, Vol. 19, No. 2, pp.192–195, https://doi.org/10.1002/ceat.270190213.

Reese, M., Marquart, C., Malmali, M., Wagner, K., Buchanan, E., McCormick, A. and Cussler, E.L. (2016) 'Performance of a small-scale Haber process', *Industrial & Engineering Chemistry Research*, Vol. 55, No. 13, pp.3742–3750, https://doi.org/10.1021/acs.iecr.5b04909.

Renner, J.N., Greenlee, L.F., Ayres, K.E. and Herring, A.M. (2015) 'Electrochemical synthesis of ammonia: a low pressure, low temperature approach', *Interface Magazine*, Vol. 24, No. 2, pp.51–57, https://doi.org/10.1149/2.f04152if.

Rouwenhorst, K.H.R., van der Ham, A.G.J., Mul, G. and Kersten, S.R.A. (2019) 'Islanded ammonia power systems: technology review & conceptual process design', *Renewable and Sustainable Energy Reviews*, Vol. 114, 109339, https://doi.org/10.1016/j.rser.2019.109339.

Sato, N. (2004) *Chemical Energy and Exergy*, Elsevier, Amsterdam, The Netherlands.

Siemens Energy (2020) *Green AMMONIA* [online] https://www.siemens-energy.com/uk/en/offerings-uk/green-*ammonia*.html (accessed 5 December 2022).

Smith, C., McCormick, A.V. and Cussler, E.L. (2019) 'Optimizing the conditions for ammonia production using absorption', *ACS Sustainable Chemistry & Engineering*, Vol. 7, No. 4, pp.4019–4029, https://doi.org/10.1021/acssuschemeng.8b05395.

Stephens, A.D. and Richards, R.J. (1973) Steady state and dynamic analysis of an ammonia synthesis plant', *Automatica,* Vol. 9, No. 1, pp.65–78, https://doi.org/10.1016/0005-1098(73)90013-7.

Szargut, J., Morris, D.R. and Steward, F.R. (1988) *Exergy Analysis of Thermal, Chemical and Metallurgical Processes*, Hemisphere Publ. Corp; Springer, New York/Washington/Philadelphia/London/Berlin/Heidelberg/New York/London/Paris/Tokyo.

Tancock, A. (2020) 'Green ammonia at oil & gas scale', *Conference Talk at the 2020 Ammonia Energy Association Conference* [online] https://www.ammoniaenergy.org/wp-content/uploads/2020/12/Alex-Tancock-Keynote.pdf (accessed 1 December2022).

Taruishi, K. (2020) De-carbonization of ocean-going vessels ', *Conference Talk at the 2020 Ammonia Energy Association Conference* [online] https://www.ammoniaenergy.org/wp-content/uploads/2020/12/Kazumasa-Taruishi.pdf (accessed 1 December 2022).

Teo, A. (2020) 'Ammonia infrastructure. Ammonia as alternative maritime fuel', *Conference Talk at the 2020 Ammonia Energy Association Conference* [online] https://dev.ammoniaenergy.org/wp-content/uploads/2020/12/Anthony-Teo.pdf (accessed 1 December 2022).

Tian, W.D., Yu, Z.P. and Sun, S.L. (2011) 'Dynamic simulation of ammonia synthesis loop under abnormal conditions', *Advanced Materials Research*, Vols. 396–398, pp.955–958, https://doi.org/10.4028/www.scientific.net/AMR.396-398.955.

Travis, A.S. (2018) *Nitrogen Capture*, Springer International Publishing, Cham.

Tripodi, A., Compagnoni, M., Bahadori, E. and Rossetti, I. (2018) 'Process simulation of ammonia synthesis over optimized Ru/C catalyst and multibed Fe + Ru configurations', *Journal of Industrial and Engineering Chemistry*, Vol. 66, pp.176–186, https://doi.org/10.1016/j.jiec.2018.05.027.

Tsatsaronis, G. (2007) 'Definitions and nomenclature in exergy analysis and exergoeconomics', *Energy*, Vol. 32, No. 4, pp.249–253, https://doi.org/10.1016/j.energy.2006.07.002.

Tsatsaronis, G. and Morosuk, T. (2008a) 'A general exergy-based method for combining a cost analysis with an environmental impact analysis: part I – theoretical development', in *Volume 8: Energy Systems: Analysis, Thermodynamics and Sustainability; Sustainable Products and Processes, ASME 2008 International Mechanical Engineering Congress and Exposition*, ASMEDC, Boston, Massachusetts, USA, 31 October–6 November, pp.453–462.

Tsatsaronis, G. and Morosuk, T. (2008b) 'A general exergy-based method for combining a cost analysis with an environmental impact analysis: part II – application to a cogeneration system', in *Volume 8: Energy Systems: Analysis, Thermodynamics and Sustainability; Sustainable Products and Processes, ASME 2008 International Mechanical Engineering Congress and Exposition*, ASMEDC, Boston, Massachusetts, USA, 31 October–6 November, pp.463–469.

Tsatsaronis, G. and Winhold, M. (1985) 'Exergoeconomic analysis and evaluation of energy-conversion plants – I. A new general methodology', *Energy*, Vol. 10, No. 1, pp.69–80, https://doi.org/10.1016/0360-5442(85)90020-9.

Uniper SE (2022) *EverWind Secures Offtake from Key German Partner Uniper for Canada's First Green Hydrogen Hub in Nova Scotia* [online] https://www.uniper.energy/news/everwind-secures-offtake-from-key-german-partner-uniper-for-canadas-first-green-hydrogen-hub-in-nova-scotia (accessed 5 December 2022).

Valera-Medina, A. and Banares-Alcantara, R. (2021) *Techno-Economic Challenges of Green Ammonia as Energy Vector*, Elsevier Science & Technology, San Diego.

Valera-Medina, A., Xiao, H., Owen-Jones, M., David, W.I.F. and Bowen, P.J. (2018) 'Ammonia for power', *Progress in Energy and Combustion Science*, Vol. 69, pp.63–102, https://doi.org/10.1016/j.pecs.2018.07.001.

Verleysen, K., Coppitters, D., Parente, A., Paepe, W.D. and Contino, F. (2020) 'How can power-to-ammonia be robust? Optimization of an ammonia synthesis plant powered by a wind turbine considering operational uncertainties', *Fuel*, Vol. 266, 117049, https://doi.org/10.1016/j.fuel.2020.117049.

Verleysen, K., Parente, A. and Contino, F. (2021) 'How sensitive is a dynamic ammonia synthesis process? Global sensitivity analysis of a dynamic Haber-Bosch process (for flexible seasonal energy storage)', *Energy*, Vol. 232, 121016, https://doi.org/10.1016/j.energy.2021.121016.

Wang, L., Xia, M., Wang, H., Huang, K., Qian, C., Maravelias, C.T. and Ozin, G.A. (2018) 'Greening ammonia toward the solar ammonia refinery', *Joule*, Vol. 2, No. 6, pp.1055–1074, https://doi.org/10.1016/j.joule.2018.04.017.

Zhang, C., Vasudevan, S. and Rangaiah, G.P. (2010) 'Plantwide control system design and performance evaluation for ammonia synthesis process', *Industrial & Engineering Chemistry Research*, Vol. 49, No. 24, pp.12538–12547, https://doi.org/10.1021/ie101135t.

Nomenclature

Symbols	
Ar	Argon
C-1	Compressor (novel layout)
	Inlet compressor (conventional layout)
C-2	Recycle compressor (conventional layout)
CH_4	Methane
COP	Coefficient of performance
E-1	Electrical preheater (novel layout)
	Internal heat exchanger (conventional layout)
EoS	Equation of state
EU	European Union
H_2	Hydrogen
HYSPR-mp	Aspen HYSYS® Peng Robinson modified binary interaction parameters
I, II, …, XII	Stream numbering
I-1	Purge valve (novel and conventional layout)
I-2	Recycle valve (novel layout)
LLHW	Langmuir Hinshelwood Hougen Watson
M-1	Mixer (novel and conventional layout)
N_2	Nitrogen
NH_3	Ammonia
P2A	Power-to-ammonia
PR	Peng Robinson
R-1	First reactor section (novel and conventional layout)
R-2	Second reactor section (novel and conventional layout)

Nomenclature (continued)

R-3	Third reactor section (novel and conventional layout)	
RK	Redlich Kwong	
RKS	Redlich Kwong Soave	
RKS-BM	Redlich Kwong Soave Boston Mathias	
S-1	Splitter (novel and conventional layout)	
SRK	Soave Redlich Kwong	
V-1	Condenser (novel and conventional layout)	
VCR	Vapour compression refrigeration	
Mathematical symbols		
$\overline{e}$	Molar total exergy	kJ/kmol
$\dot{E}$	Total exergy flow	kJ/hr
$\overline{g}$	Molar Gibbs energy (free enthalpy)	kJ/kmol
$\Delta\overline{h}^{\circ}$	Molar standard reaction enthalpy (1.01325 bar, 298 K)	kJ/mol
$\dot{M}$	Mass flow	kg/hr
$\dot{N}$	Mole flow	kmol/hr
p	Pressure	bar
P	Power	MJ/hr
$\dot{Q}$	Heat/cooling stream	MJ/hr
$\overline{R}$	Molar gas constant	kJ/(kmol·K)
T	Temperature	°C, K
y	Mole fraction	-, %
Greek symbols		
ϵ	Exergetic degree of efficiency	-, %
ξ	Exergy destruction over total exergy fuel	-, %
ϕ	Exergy destruction over total exergy destruction	-, %
Superscripts		
CH	Chemical	
e	Excess	
m	Counting limit for number of unit operations	
n	Counting limit for number of components	
PH	Physical	
Subscripts		
0	Ambient	
D	Destruction	
el	Electric	
F	Fuel	
i	Stream number, i = I, II, …, XII	

Nomenclature (continued)

Subscripts	
id	Ideal
j	Component, j = H_2, N_2 and NH_3
k	Unit operation number/name, k = M-1, C-1, …, I-2
l	Liquid
L	Loss
Mix	Mixture
P	Product
Q	Heat
sb	System boundary
tot	Total
W	Work